Post-Processing for Spectral Coherence of Magnetoencephalogram Background Activity: Application to Alzheimer's Disease

Javier Escudero[1], *Member, IEEE*, Athanasios Anastasiou[2], and Alberto Fernández[3]

***Abstract*— Estimating the connectivity between magnetoencephalogram (MEG) signals provides an excellent opportunity to analyze whole brain functional integration across a spectrum of conditions from health to disease. For this purpose, spectral coherence has been used widely as an easy-to-interpret metric of signal coupling. However, a number of systematic effects may influence the estimations of spectral coherence and subsequent inferences about brain activity. In this pilot study, we focus on the potentially confounding effects of the field spread and the on-going dynamic temporal variability inherent in the signals. We propose two simple post-processing approaches to account for these: 1) a jack-knife procedure to account for the variance in the estimation of spectral coherence; and 2) a detrending technique to reduce its dependence on sensor proximity. We illustrate the effect of these techniques in the estimation of MEG spectral coherence in the α band for 36 patients with Alzheimer's disease and 26 control subjects.**

I. Introduction

The brain activity can be recorded non-invasively by means of the electroencephalogram (EEG) and magnetoencephalogram (MEG). These recordings have high temporal resolution, orders of magnitude better than other methods for quantifying cerebral activity such as positron emission tomography or functional magnetic resonance imaging. In addition, the MEG is reference-free and less affected by the extra-cerebral tissues than the EEG [1].

Traditionally, EEG and MEG data have been analyzed on a channel-by-channel basis [2], [3]. By focusing on the characteristics of individual channels and ignoring their interaction, these approaches have limited ability to characterise whole-brain function and they fail to capture the characteristics of functional integration, which refers to statistical dependencies, or coupling, between spatially distinct brain signals [4]. There is growing evidence that the evaluation of functional integration in EEG and MEG may help in the characterization of pathology and other brain conditions [5].

Functional integration has traditionally been assessed using spectral coherence, $coh(\cdot)$, a widespread metric that assesses linear dependences between two signals via the frequency domain [5], [6]. Spectral coherence suffers, however, from bias as a result of field spread. Various other functional integration metrics have been proposed as alternatives (e.g., phase lag index, PSI) [7], [8]. Nevertheless, the results of spectral coherence are highly correlated with those of many other functional integration metrics used in the literature [5]. This fact, together with its simplicity of interpretation, still makes spectral coherence a relevant option for the estimation of brain functional integration in disease and mental states.

In addition, recent evidence suggests that the characteristics of resting state functional integration change dynamically with time [4], [9]. This fact may introduce a certain level of variability in the dominating pattern of functional integration associated with resting state. Furthermore, previous analyses have suggested that the features computed from MEG activity of Alzheimer's disease (AD) patients might have different levels of variability (as measured by standard deviation, SD) in comparison with those of control subjects [10].

Considering these facts, we theorize that functional integration derived from MEG signals using some coupling metric C may contain contributions from several underlying effects. To make this more specific, consider the ordered set of acquired MEG signals $\mathbf{X} \in \{x_{k,n} \in \mathbb{R}\}$ with $k \in [1, \ldots, N_{Channels}]$ and $n \in [1, \ldots, N_{Samples}]$ where $N_{Channels}$, $N_{Samples}$ denote the total number of MEG channels and samples acquired at a sampling frequency F_s, respectively. We assume that the functional integration, as estimated by C, 'encodes', as a function $g[\cdot]$, the following:

$$\begin{aligned} C_{Meas}(i,j,f) = \ldots \\ g[C_{Con}(i,j,f), C_{Exp}(i,j,f), C_{Dist}(i,j,f)] + \epsilon, \end{aligned} \quad (1)$$

where $C_{Meas}(i,j,f)$ is the measured functional integration, ϵ accounts for effects external to this model, and $C_{Con}(i,j,f)$, $C_{Exp}(i,j,f)$, $C_{Dist}(i,j,f)$ represent the contributions of the disease (or mental condition being evaluated), the experimental paradigm (e.g., resting state and/or variability in the signals), and the distance between sensors (in relation to the field spread), respectively. $i,j \in [1, \ldots, N_{Channels}]$ denote two distinct signals and f represents frequency.

Based on Eq. (1), we propose two simple post-processing approaches to account for the confounding effects induced in the estimated levels of functional integration (C_{Meas}) by the potential temporal variability in resting state activity (C_{Exp}) and the field spread (C_{Dist}). These post-processing approaches are based on applying a jack-knife procedure to normalize the coupling values by estimations of their

[1]Javier Escudero is with the Institute for Digital Communications, School of Engineering, University of Edinburgh, Edinburgh, King's Buildings, EH9 3JL, UK. (Phone: +44 131 650 599; Email: javier.escudero@ed.ac.uk, javier.escudero@ieee.org)

[2]Athanasios Anastasiou is with the College of Medicine, Swansea University, Swansea, UK. (A.Anastasiou@swansea.ac.uk)

[3]Alberto Fernández is with the Departamento de Psiquiatría y Psicología Médica, Universidad Complutense de Madrid, Madrid, Spain. He is also with Laboratorio de Neurociencia Cognitiva y Computacional, Centro de Tecnología Biomédica, Universidad Politécnica de Madrid and Universidad Complutense de Madrid, Madrid, Spain and with the Insitituto de Investigación Sanitaria San Carlos (IdSSC).

978-1-4244-7929-0/14/$26.00 ©2014 IEEE

variance and on detrending the effect of inter-sensor distance from the estimated functional integration levels.

These post-processing techniques can easily be applied to already computed coupling metrics. We illustrate them by analyzing the $coh(\cdot)$ in the α band (8Hz-13Hz) of resting state MEG activity of 36 patients with AD and 26 control subjects. AD is a particularly relevant disease for this study due to its huge societal impact [11] and the fact that it has been hypothesized to be a disconnection syndrome [6], [12].

II. Materials

A. Subject groups

MEG resting state activity was acquired from 36 AD patients and 26 age-matched controls (CON). All subjects gave their informed consent for the research, which was approved by the local ethics committee. Diagnoses were confirmed with thorough tests. The mini-mental state examination (MMSE) was used to screen the cognitive status [6].

The 36 AD patients (24 females) met the criteria for probable AD according to the guidelines of the NINCDS-ADRDA [13]. Their mean age and MMSE score were 74.06 ± 6.95 years and 18.06 ± 3.36, in that order (mean$\pm$SD).

The 26 CON subjects (17 females) were 71.77 ± 6.38 years old (mean$\pm$SD). Their MMSE score was 28.88 ± 1.18 (mean$\pm$SD). The difference in age between groups was not significant (p-value = 0.1911, Student's t-test).

B. MEG Recordings

Resting state MEG activity was acquired with a 148-channel whole-head magnetometer (MAGNES 2500 WH, 4D Neuroimaging) in a magnetically shielded room at the MEG Centre Dr. Pérez-Modrego (Spain). The subjects lied on a patient bed with eyes closed in relaxed state. They were asked to stay awake and not to move eyes and head. For each participant, five minutes of MEG resting state activity were recorded at F_s=169.54Hz. The signals were split into epochs of 10s and visually inspected with the aid of an automated thresholding procedure to discard epochs severely contaminated with artefacts [6]. The cardiac artifact was removed from the signals using a constraint blind source separation procedure [14] to avoid bias in the computation of signal coupling [6]. Finally, a bandpass FIR filter with cut-offs at 1.5Hz and 40Hz was applied the recordings.

III. Methods

We investigate the ability of spectral coherence, $coh(x_u, x_v, f)$, as a metric of functional integration between two MEG channels, $x_u, x_v \in \mathbf{X}$, computed in the α band ($f \in [8\text{Hz}, 13\text{Hz}]$) to distinguish AD from CON subjects with and without two post-processing stages that try to account for the confounding effects hypothesized in Eq. (1).

We first compute $coh(x_u, x_v, f)$ for each artefact-free epoch of each subject [5], [6] as indicated in Section III-A. Then, we apply two different post-processing schemes. The first one, described in Section III-B, is a jack-knife approach to normalize the values of $coh(x_u, x_v, f)$. The second, described in Section III-C, tries to counteract the dependence of $coh(x_u, x_v, f)$ on the distance between channels, u, v.

After each stage, we evaluate the ability to discriminate AD from CON subjects via the p-values of a Mann-Whitney U-test for each pair of channels adjusted for False Discovery Rate (FDR) to account for multiple tests [16].

A. Computation of spectral coherence

Spectral coherence – $coh(x_u, x_v, f)$ – is a widespread and easy-to-interpret measure of brain synchrony [5], [6]. It measures linear correlation between two time-series (x_u, x_v) as a function of frequency. Its values range from 0 (no correlation) to 1 (maximum correlation). $coh(x_u, x_v, f)$ estimates linear synchrony between signals but it cannot discern the direction of the coupling [5], [6]. It is strongly correlated with other commonly used synchronization metrics [5].

To calculate spectral coherence, two time series of equal length – x_u and x_v – are split into B equal blocks of 2s each with 50% overlap. It is then estimated via:

$$coh(x_u, x_v, f) = \frac{|\langle X_u(f) X_v^*(f) \rangle|^2}{|\langle X_u(f) \rangle||\langle X_v(f) \rangle|}, \tag{2}$$

where $X_u(f)$ and $X_v(f)$ are the frequency spectra of x_u, x_v, respectively (including a Hanning window to each block). * indicates complex conjugate, $|\cdot|$ is magnitude, and $\langle \cdot \rangle$ denotes averaging over the B blocks [5], [6]. The computations were carried out using FieldTrip [15].

B. Jack-knife for variability estimation

Jack-knife is a procedure similar to bootstrapping to estimate the variance of a statistic. It was proposed to normalise the estimations of the PSI in [8]. We use a similar approach to take into account the variability across signal epochs that may be present due to changes in the experimental conditions – conceptualized in $C_{Exp}(i, j, f)$ in Eq. (1). This leads to normalized values of spectral coherence – $coh_{Norm}(x_u, x_v, f)$ – as follows:

$$coh_{Norm}(x_u, x_v, f) = \frac{coh(x_u, x_v, f)}{std[coh(x_u, x_v, f)]}, \tag{3}$$

where $coh(x_u, x_v, f)$ refers to the average value of spectral coherence across all epochs of a subject and $std[coh(x_u, x_v, f)]$ is the standard deviation computed with a jack-knife approach [8]. This is done by creating as many replicates, $coh_e(x_u, x_v, f)$, of the spectral coherence as artifact-free epochs in the data, E, each of which has the e^{th} epoch removed. $std[coh(x_u, x_v, f)]$ is calculated as $\sqrt{E}\sigma$ with σ being the standard deviation of the set of $coh_e(x_u, x_v, f)$ [8].

C. Detrending

Detrending refers to the process of removing a slowly varying trend from a quantity. In the field of biomedical signal processing, detrending is used to remove slowly varying components from signals such as the electrocardiogram [17] and the EEG [18]. This is usually done by fitting a low order polynom to the data and then subtracting the trend

represented by the polynom from it. In this study, we employ the idea of detrending to remove the spatial cofactor between the coherence of any two $x_u, x_v \in \mathbf{X}$ that may appear in the results due to the field spread.

The proposed algorithm requires knowledge of the physical locations of the u, v MEG sensors. Assuming that this is provided in some $L \in \{l_k \in \mathbb{R}^3, k \in [1, \ldots, N_{Channels}]\}$, the coherence estimates are detrended as follows:

Algorithm 1 Spectral coherence detrending

Input: $\mathbf{X}, L, f$

Output: $\mathbf{W}$ {Detrended values}

$S \leftarrow \{u \times N_{Channels} + v \; \forall \; u, v \in [1, \ldots, N_{Channels}]\}$

$M \leftarrow \{m_s = coh(x_u, x_v, f), s \in S, x \in \mathbf{X}\}$

$D \leftarrow \{d_s = \|l_u - l_v\|, s \in S, l \in L\}$

$q \leftarrow polyfit(D, M, 7)$

$\mathbf{W} \leftarrow \{w_{u,v} = m_s - polyval(q, d_s), s \in S, m \in M, d \in D\}$

return $\mathbf{W}$

The functions $polyfit(D, M, order)$ and $polyval(q, d_s)$ abstract the fitting of a polynomial (q) of some order $order$ and its evaluation at some d_s, respectively. Here, $order = 7 \ll N^2_{Channels}$ as 7th order was deemed satisfactory for the purposes of this study after visual inspection of the prevailing form of the relationship between distance and $coh(x_u, x_v, f)$ averaged over the CON subjects.

It is possible to apply Algorithm 1 to each individual subject in an attempt to counteract the C_{Dist} effect in Eq. (1). However, in this study, we adopt the alternative approach of deriving a q from the average coherence estimates (M) of all CON subjects and then use it to detrend both AD and CON subsets because the effect of disease on coherence (C_{Con}) seems to be weaker than the effect of distance (C_{Dist}). In this way, we try to reduce the effect of sensor proximity but still maintain the differentiating elements in the connectivity patterns across the groups. Computing the polynomial fitting from all CON subjects has the added benefit of providing a detrending polynom that could be applied without modification to other clinical populations.

IV. Results and Discussion

The effect of the post-processing was evaluated via a set of individual FDR-adjusted [16] Mann-Whitney U-tests.

The p-values for the differences in the level of $coh(x_u, x_v, f)$ in the α band at each pair of MEG channels without any post-processing at all are shown in Fig. 1. The differences are not significant for any pair of channels (light and red colors indicate p-values > 0.05).

Similarly, Fig. 2 depicts the p-values for spectral coherence after applying the jack-knife technique (i.e., coh_{Norm}) where, overall, the differences between subject groups are far more pronounced (darker colors than in Fig. 1), with most pairs of MEG channels having p-values < 0.05.

Fig. 3 depicts the dependence of spectral coherence on sensor proximity for one CON subject in both previous situations: without any post-processing (coh, top panel) and with the jack-knife-based post-processing (coh_{Norm}, bottom

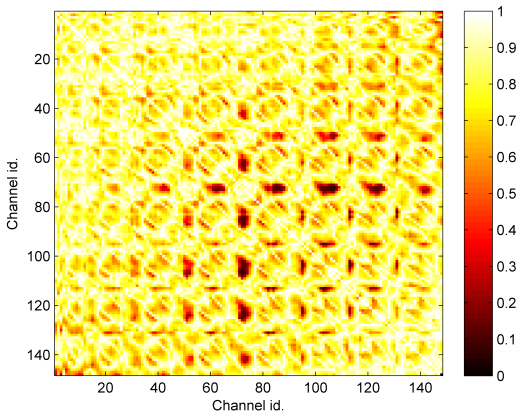

Fig. 1. FDR-adjusted Mann-Whitney U-test p-values for spectral coherence, $coh(x_u, x_v, f)$, in the α band.

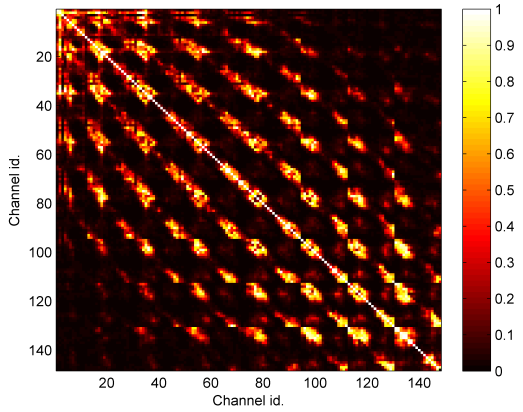

Fig. 2. FDR-adjusted Mann-Whitney U-test p-values for spectral coherence after post-processing with jack-knife, $coh_{Norm}(x_u, x_v, f)$, in the α band.

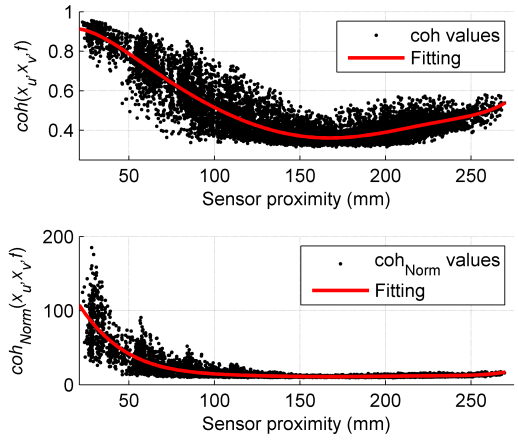

Fig. 3. Example of the spectral coherence dependence on sensor proximity without any post-processing (top) and after employing jack-knife (bottom) for a CON subject in the α band. The polynomial fitting computed for that CON subject is also illustrated as an example.

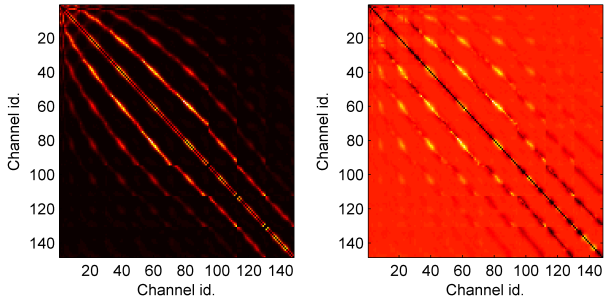

Fig. 4. Example of the level of spectral coherence in the α band after jack-knife only (left) and after jack-knife and detrending (right) for one CON subject (lighter colors indicate higher coherence).

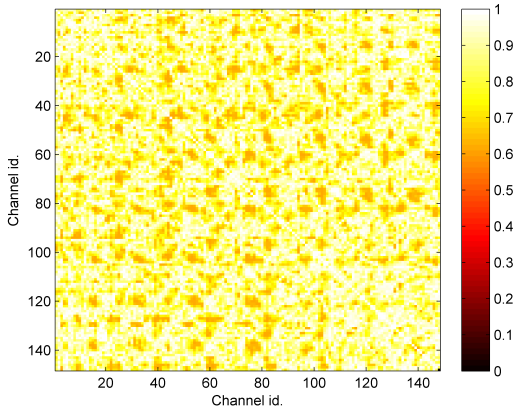

Fig. 5. FDR-adjusted Mann-Whitney U-test p-values for PSI in α.

panel). As expected, a strong proximity dependency can still be observed after jack-knifing as this procedure does not intend to tackle the effect of channel proximity. Fig. 3 also depicts an example of the polynomial fitting that would have been computed for that CON subject, as an example.

To account for this dependency, we applied detrending. As the same detrending was applied to each pair of channels for all subjects, the p-values for differences between subject groups are the same as in Fig. 2. Nonetheless, detrending may still be valuable in reducing spurious highly correlated clusters of closely placed sensors and, thereby, in improving whole-brain analysis using graph theory (as in [4]). Indicative global changes of coupling between all channels are illustrated in Fig. 4 for the same subject as depicted in Fig. 3.

Compared to other coupling metrics such as PSI, our results suggest that the post-processed spectral coherence might be sensitive to differences between AD and CON subjects, as this dementia affects the brain functional connectivity [5], [6], [12]. The comparison with PSI is illustrated in Fig. 5 which depicts the p-values for the PSI in the α band (using the full method in [8]).

V. Conclusion

This pilot study described two straightforward post-processing approaches that are here combined for the first time to account for the confounding effects hypothesized in Eq. (1). Jack-knifing seemed to enhance the differences between subject groups (due to reducing the variability in the coherence) whereas Detrending might improve whole-brain graph theory analysis. Future analyses will try to corroborate these findings applying graph theory analysis to other spectral bands and diseases although we acknowledge that they may be limited by the lack of ground truth.

References

[1] F. Lopes da Silva, "EEG and MEG: Relevance to Neuroscience," *Neuron*, vol. 80, no. 5, pp. 1112-1128, Dec. 2013.

[2] R. Hornero, D. Abásolo, J. Escudero, and C. Gómez, "Nonlinear analysis of electroencephalogram and magnetoencephalogram recordings in patients with Alzheimers disease," *Philos. Trans. R. Soc. Math. Phys. Eng. Sci.*, vol. 367, no. 1887, pp. 317-336, Jan. 2009.

[3] C. J. Stam, "Use of magnetoencephalography (MEG) to study functional brain networks in neurodegenerative disorders," *J. Neurol. Sci.*, vol. 289, no. 1-2, pp. 128-134, Feb. 2010.

[4] A. Fornito, A. Zalesky, and M. Breakspear, "Graph analysis of the human connectome: Promise, progress, and pitfalls," *NeuroImage*, vol. 80, pp. 426-444, Oct. 2013.

[5] J. Dauwels, F. Vialatte, T. Musha, and A. Cichocki, "A comparative study of synchrony measures for the early diagnosis of Alzheimers disease based on EEG," *NeuroImage*, vol. 49, no. 1, pp. 668-693, Jan. 2010.

[6] J. Escudero, S. Sanei, D. Jarchi, D. Abásolo, and R. Hornero, "Regional coherence evaluation in mild cognitive impairment and Alzheimers disease based on adaptively extracted magnetoencephalogram rhythms," *Physiol. Meas.*, vol. 32, no. 8, pp. 1163-1180, Aug. 2011.

[7] L. J. Larson-Prior, R. Oostenveld, S. Della Penna, G. Michalareas, F. Prior, A. Babajani-Feremi, et al., "Adding dynamics to the Human Connectome Project with MEG," *NeuroImage*, vol. 80, pp. 190-201, Oct. 2013.

[8] G. Nolte, A. Ziehe, V. V. Nikulin, A. Schlögl, N. Krämer, T. Brismar, and K.-R. Müller, "Robustly Estimating the Flow Direction of Information in Complex Physical Systems," *Phys. Rev. Lett.*, vol. 100, no. 23, p. 234101, Jun. 2008.

[9] S. Mehrkanoon, M. Breakspear, and T. W. Boonstra, "Low-Dimensional Dynamics of Resting-State Cortical Activity," *Brain Topogr.*, vol. 27, no. 3, pp. 338-352, May 2014.

[10] J. Poza, R. Hornero, J. Escudero, A. Fernández, and C. Gómez, "Analysis of spontaneous MEG activity in Alzheimers disease using time-frequency parameters," in 30th Annual International Conference of the IEEE Engineering in Medicine and Biology Society, 2008, pp. 5712-5715.

[11] A. Wimo and M. Prince, "World Alzheimer Report 2010: The global economic impact of dementia," Alzheimers Disease International, Sep. 2010.

[12] J. Jeong, "EEG dynamics in patients with Alzheimers disease," *Clin. Neurophysiol.*, vol. 115, no. 7, pp. 1490-1505, Jul. 2004.

[13] G. McKhann, D. Drachman, M. Folstein, R. Katzman, D. Price, and E. M. Stadlan, "Clinical diagnosis of Alzheimers disease: Report of the NINCDS-ADRDA Work Group under the auspices of Department of Health and Human Services Task Force on Alzheimers Disease," *Neurology*, vol. 34, no. 7, pp. 939-944, 1984.

[14] J. Escudero, R. Hornero, D. Abásolo, and A. Fernández, "Quantitative Evaluation of Artifact Removal in Real Magnetoencephalogram Signals with Blind Source Separation," *Ann. Biomed. Eng.*, vol. 39, no. 8, pp. 2274-2286, 2011.

[15] R. Oostenveld, P. Fries, E. Maris, and J.-M. Schoffelen, "FieldTrip: Open Source Software for Advanced Analysis of MEG, EEG, and Invasive Electrophysiological Data," *Comput. Intell. Neurosci.*, vol. 2011, p. 156869, Dec. 2010.

[16] Y. Benjamini and Y. Hochberg, "Controlling the False Discovery Rate: A Practical and Powerful Approach to Multiple Testing," *J. R. Stat. Soc. Ser. B Stat. Methodol.*, vol. 57, no. 1, pp. 289-300, Jan. 1995.

[17] D. A. Litvack, T. F. Oberlander, L. H. Carney, and J. P. Saul, "Time and frequency domain methods for heart rate variability analysis: a methodological comparison," *Psychophysiology*, vol. 32, no. 5, pp. 492-504, Sep. 1995.

[18] C. J. Stam, T. Montez, B. F. Jones, S. A. R. B. Rombouts, Y. van der Made, Y. A. L. Pijnenburg, and P. Scheltens, "Disturbed fluctuations of resting state EEG synchronization in Alzheimers disease," *Clin. Neurophysiol.*, vol. 116, no. 3, pp. 708-715, Mar. 2005.